

Efficient Implementation of Quasi-Maximum-Likelihood Detection Based on Semidefinite Relaxation

Mikalai Kisialiou, Xiaodong Luo, and Zhi-Quan Luo, *Fellow, IEEE*

Abstract—In this paper we develop two quasi-Maximum Likelihood channel detectors for multiuser detection: SDR detector and PSK detector. These detectors can deliver near-ML BER performance with a polynomial worst-case complexity. The SDR detector for BPSK constellation is based on a convex semidefinite relaxation, whereas the PSK detector for M -PSK constellations is based on a non-convex low-rank semidefinite relaxation. The SDR detector is implemented using a dual-scaling interior-point method, while the PSK detector is based on a coordinate descent strategy on a feasible region homotopy. We use dynamic dimension reduction and warm start techniques to achieve SNR-sensitive improvements for both detectors. Numerical simulations of BER performance and running time indicate the effectiveness of the two quasi-ML detectors when compared to the conventional sphere decoder and its variants.

Index Terms—Dimension reduction, duality, maximum-likelihood detection, MIMO systems, semidefinite relaxation.

I. INTRODUCTION

CONSIDER a vector communication channel with n transmit and m receive antennas:

$$\mathbf{y} = \sqrt{\rho} \mathbf{H} \mathbf{s} + \mathbf{v}, \quad (1)$$

where ρ denotes the Signal-to-Noise Ratio (SNR) at each receiver; $\mathbf{s} = (s_1, \dots, s_n)^\dagger \in \mathcal{C}^n$ is a vector of transmitted symbols drawn from a constellation set \mathcal{C}^n , $(\cdot)^\dagger$ denotes matrix transpose (Hermitian transpose for complex values); \mathbf{H} is an $m \times n$ channel matrix with i.i.d. entries; \mathbf{v} is a Gaussian noise vector with i.i.d. entries; and \mathbf{y} is a vector of received signals. We consider model (1) with a general class of random channels, normalized so that

$$\begin{aligned} E\{s_k\} &= 0, & E\{|s_k|^2\} &= 1, & \forall k, \\ E\{H_{ik}\} &= 0, & E\{|H_{ik}|^2\} &= 1/n, & \forall i, k, \\ E\{v_i\} &= 0, & E\{|v_i|^2\} &= 1, & \forall i, \end{aligned} \quad (2)$$

where $E\{\cdot\}$ denotes expectation. In this paper we focus on two signal constellations, Quadrature Amplitude Modulation (QAM) and Phase Shift Keying (PSK). Both constellations are common in practical applications: QAM constellations are widely used in high-rate communication systems, while PSK

Manuscript received March 22, 2007; revised August 27, 2008. This research is supported in part by the National Science Foundation, Grant No. DMS-0610037. A preliminary version of this paper was published in the Proceedings of ICASSP'03, Hong Kong and the Proceedings of ICASSP'05, Philadelphia, U.S.A.

M. Kisialiou and Z.-Q. Luo are with the Department of Electrical and Computer Engineering, University of Minnesota. X. Luo is with Sabre Airline Solutions, Inc.

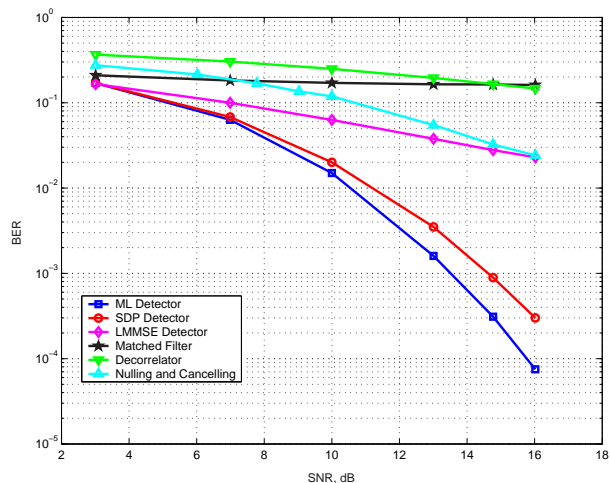


Fig. 1. BER performance of various detectors, $n = m = 10$, BPSK.

constellations are popular because they allow a simple signal amplifier design and can be used in differential modulation schemes.

The maximum-likelihood (ML) detection is known to deliver optimal block error rate performance. For Gaussian noise, ML detection can be written as the following Integer Least-Squares problem:

$$\mathbf{s}_{ML} = \arg \min_{\mathbf{s} \in \mathcal{C}^n} \|\mathbf{y} - \sqrt{\rho} \mathbf{H} \mathbf{s}\|^2. \quad (3)$$

This problem is known to be NP-hard. For small problem size the exhaustive search can be used to solve (3). However, for large systems this approach becomes prohibitively expensive.

The popular sphere decoding algorithm can deliver the ML-like BER performance with significantly reduced complexity compared to the brute force ML detector. It was first introduced in [7] and later studied extensively in literature; see [6], [8, Chapter 5], [26] and references therein. **The sphere decoder is a variant of tree search detectors [19] that restricts** the exhaustive search to an ellipsoid centered at the zero-forcing estimate, $\mathbf{s}_{ZF} = (1/\sqrt{\rho}) (\mathbf{H}^\dagger \mathbf{H})^{-1} \mathbf{H}^\dagger \mathbf{y}$. In high SNR region, this strategy allows a fast implementation since the ML solution is close to \mathbf{s}_{ZF} with high probability. Unfortunately, the sphere decoder still suffers from exponential complexity [11], and exhibits poor empirical performance in low SNR region or for large problems. In addition, the running time of the sphere decoder can vary significantly for different channel realizations, thus making it less attractive for

embedded applications.

Alternative strategies have been developed to overcome high computational complexity of the ML detector. These detectors achieve polynomial complexity $\mathcal{O}(n^3)$ by relaxing the integer constraint in the ML detection problem (3). Such relaxation often results in a substantial deterioration of the BER performance, see Fig. 1 for the BER performance of the LMMSE detector, matched filter, decorrelator, and nulling and cancelling strategy.

In this paper we focus on the quasi-ML detectors unifying the two advantages of polynomial complexity and near-optimal BER performance. A prominent detector in this category was introduced [16], [24]. This detector is based on a convex semidefinite relaxation of the ML detection problem, followed by a (randomized) rounding procedure. It enjoys excellent BER performance, see Fig. 1. Interior-point methods can be used to implement this strategy with polynomial worst-case complexity for detection of BPSK signals [16], QAM signals [5], [17], [18], [22], [27], [28], or PSK signals [13], [15], [20]. The running time of existing semidefinite relaxation detectors scales well with the problem size and is insensitive to SNR. This insensitivity is a blessing in low SNR region where the ML detection problem is more difficult. However, it becomes a curse in high SNR region since it implies the algorithm fails to effectively exploit the low noise property of the channel, as does the sphere decoder. Another drawback of the current implementations is the lack of an efficient termination procedure. All symbols are rounded simultaneously in the end, irrespective of their reliabilities. In this work we present theoretical analysis and efficient implementations of two quasi-ML detectors which overcome the drawbacks stated above.

For BPSK-modulated signals, we develop a quasi-ML detector based on a convex semidefinite relaxation [16], called the SDR detector hereafter. For a general class of random channels (1) and (2), theoretical analysis based on random matrix theory [12] shows that the SDR detector provides a constant factor approximation of the log-likelihood value for the ML detection problem in probability and delivers the exact ML solution in high SNR region. We present an efficient implementation of the SDR detector which empirically achieves near-optimal BER performance with polynomial complexity. The core of the proposed implementation is a dual-scaling interior-point algorithm [2]. A warm start technique, implemented with a truncated version of the sphere decoder, provides an SNR-sensitive initialization. The standard randomized rounding step is replaced with a dynamic dimension reduction technique which gradually rounds the symbols with high reliability and reduces problem size at every iteration of the dual-scaling algorithm.

For PSK-modulated signals, we propose a low-rank (non-convex) semidefinite relaxation [4] for the ML detection problem, and an efficient implementation of the quasi-ML detector, called the PSK detector hereafter. Theoretical analysis of this low-rank non-convex relaxation [13] shows that the PSK detector delivers a $\frac{1}{2}$ -maximizer of the original ML detection problem, and the global maximizer when input is BPSK. The core of the PSK detector is a coordinate descent method

implemented over a homotopy of a relaxed feasible set. A warm start procedure and a dynamic dimension reduction technique allow us to make efficient use of symbol reliabilities to deliver highly optimized running time. The PSK detector enjoys worst-case polynomial complexity (when initialized with $\mathbf{H}^\dagger \mathbf{H}$, the remaining complexity is $\mathcal{O}(n^2)$) and scales gracefully with problem size and SNR.

We show that, in addition to popular PSK constellations, the SDR and PSK detectors can also be applied to detect signals modulated with square QAM constellations.

Monte-Carlo simulations show that for the Rayleigh fading channel with BPSK/QPSK/8-PSK/16-QAM constellations our implementations of the SDR and PSK detectors compare favorably to other existing quasi-ML detectors in terms of both BER and running time. The current versions and the subsequent improvements for the SDR and PSK detectors presented in this paper are available online [29].

II. QUASI-MAXIMUM-LIKELIHOOD DETECTION

A. Localized exhaustive search

The sphere decoder originates from an algorithm for computing the shortest vector in a lattice [7]. Various improvements [8], [26] (e.g. adjustable radius search procedure) have been proposed to adapt it to the ML detection problem, demonstrating impressive running time for small systems operating in high SNR region. However, the average and worst-case complexity of the sphere decoder is exponential [9], [11]: for any polynomial radius search procedure and for any node ordering, the number of objective function evaluations, N_f , performed by the sphere decoder is lower bounded by the exponential function in probability:

$$\lim_{n \rightarrow \infty} P \{N_f \geq \exp(\eta n)\} = 1,$$

where $\eta = \eta(\rho, \mathcal{C})$ is a positive function of SNR ρ and constellation set \mathcal{C} , and $P\{\cdot\}$ denotes probability. The exponential complexity of the sphere decoder manifests itself empirically in the form of unacceptably long running time in low SNR region for large input size.

B. Semidefinite relaxation (SDR detector)

Let $\mathcal{C}_{M\text{-PSK}}^{n+1}$ denote a discrete set of complex-valued M -PSK vectors \mathbf{x} of dimension $n+1$. For a general M -PSK constellation, the ML detection problem (3) allows an equivalent reformulation [16]:

$$f_{ML} := \min_{\mathbf{x} \in \mathcal{C}_{M\text{-PSK}}^{n+1}} \text{Trace}(\mathbf{Q}\mathbf{X}) \quad \text{s.t.} \quad \mathbf{X} = \mathbf{x}\mathbf{x}^\dagger, \quad (4)$$

where matrix \mathbf{Q} and vector \mathbf{x} are defined as follows

$$\mathbf{Q} = \begin{bmatrix} \rho \mathbf{H}^\dagger \mathbf{H} & -\sqrt{\rho} \mathbf{H}^\dagger \mathbf{y} \\ -\sqrt{\rho} \mathbf{y}^\dagger \mathbf{H} & \|\mathbf{y}\|^2 \end{bmatrix}, \quad \mathbf{x} = \begin{bmatrix} \mathbf{s} \\ 1 \end{bmatrix}. \quad (5)$$

Notice that any feasible matrix \mathbf{X} in (4) is positive semidefinite with all diagonal entries equal to 1. Define $\text{diag}(\mathbf{X})$ to be a vector with entries equal to the diagonal entries of matrix \mathbf{X} , \mathbf{e} to be an all-one vector, and let $\mathbf{X} \succeq 0$ denote a Hermitian positive semidefinite matrix \mathbf{X} . The detector [16] relaxes the last two

constraints $\{\mathbf{X} = \mathbf{x}\mathbf{x}^\dagger, \mathbf{x} \in \mathcal{C}_{M\text{-PSK}}^{n+1}\}$ to $\{\text{diag}(\mathbf{X}) = \mathbf{e}, \mathbf{X} \succeq 0\}$ which leads to a relaxation based on the (primal) convex Semidefinite Program (SDP):

$$\begin{aligned} f_{SDP}(\mathbf{X}) &:= \min \text{Trace}(\mathbf{Q}\mathbf{X}) \\ \text{s.t. } &\text{diag}(\mathbf{X}) = \mathbf{e}, \\ &\mathbf{X} \succeq 0. \end{aligned} \quad (6)$$

Various (often randomized) rounding procedures can be applied to generate an estimate of the transmitted M -PSK symbols based on the optimal solution \mathbf{X}_{opt} of (6), see [15], [16]. In this work we use the following rounding procedure, although a more general procedure for M -PSK symbols is possible [15]:

- Compute the spectral decomposition $\mathbf{X}_{opt} = \sum_{i=1}^{n+1} \lambda_i \mathbf{u}_i \mathbf{u}_i^\dagger$, where $\|\mathbf{u}_i\| = 1, \lambda_i \geq 0, i = 1, \dots, n+1$.
- Set $\mathbf{v}_i := \sqrt{\lambda_i} \mathbf{u}_i$ and pick vector \mathbf{v}^{max} that corresponds to the largest eigenvalue:

$$\mathbf{v}^{max} := \arg \max_{1 \leq i \leq n+1} \{\|\mathbf{v}_i\|\}.$$

- Rotate vector \mathbf{v}^{max} to ensure that the last entry is a positive real value, $\mathbf{v}^{max} := \mathbf{v}^{max} (v_{n+1}^{max})^* / |v_{n+1}^{max}|$, where $(\cdot)^*$ denotes complex conjugation.
- For each entry x_i define Bernoulli distribution:

$$\begin{aligned} P\{x_i = +1\} &= (1 + \text{Re}\{v_i^{max}\})/2, \\ P\{x_i = -1\} &= (1 - \text{Re}\{v_i^{max}\})/2, \end{aligned} \quad (7)$$

where $\text{Re}\{\cdot\}$ denotes the real part of a complex value.

- Generate a fixed number D (typically 5 – 10) of i.i.d. $(n+1)$ -dimensional vector samples $\bar{\mathbf{x}}_d, d = 1, \dots, D$, according to the distribution in (7).
- For all samples, set $\bar{\mathbf{x}}_d := -\bar{\mathbf{x}}_d$ if $(n+1)$ -st entry of $\bar{\mathbf{x}}_d$ is equal to -1 .
- Pick $\mathbf{x}_{SDR} := \arg \min_d \bar{\mathbf{x}}_d^\dagger \mathbf{Q} \bar{\mathbf{x}}_d$ and set the best achieved objective value:

$$f_{SDR} := \mathbf{x}_{SDR}^\dagger \mathbf{Q} \mathbf{x}_{SDR}. \quad (8)$$

- Output objective value f_{SDR} and \mathbf{s}_{SDR} which contains first n entries of vector \mathbf{x}_{SDR} .

The SDR detector presented above allows a probabilistic constant factor optimality for the ML detection problem. In particular, let f_{SDR} (f_{ML}) denote the objective value of the SDR (ML) detector, c.f. (4) and (8):

$$\begin{aligned} f_{SDR} &:= \|\mathbf{y} - \sqrt{\rho} \mathbf{H} \mathbf{s}_{SDR}\|^2, \\ f_{ML} &:= \|\mathbf{y} - \sqrt{\rho} \mathbf{H} \mathbf{s}_{ML}\|^2, \end{aligned} \quad (9)$$

where \mathbf{s}_{SDR} and \mathbf{s}_{ML} are the outputs of the SDR and ML detectors respectively. The approximation ratio of the SDR detector, defined as f_{SDR}/f_{ML} , is always lower bounded: $1 \leq f_{SDR}/f_{ML}$. In the worst case, as $n, m \rightarrow \infty$ such that $m/n \rightarrow \gamma$ for some $\gamma \geq 1$, the approximation ratio f_{SDR}/f_{ML} can grow unbounded. However, for the SDR detector theoretical analysis [12] based on random matrix theory and duality theory shows that f_{SDR}/f_{ML} is bounded in probability:

Theorem 1: Consider the general class of random channels specified by (1) and (2). For any positive constants r, κ and

$\gamma \geq 1$, the SDR detector provides a constant factor $c(\rho, \gamma)$ approximation for the ML detection problem in probability:

$$\lim_{\substack{m, n, D \rightarrow \infty \\ m/n \rightarrow \gamma, D = rn^{1+\kappa}}} P \left\{ \frac{f_{SDR}}{f_{ML}} \leq c(\rho, \gamma) \right\} = 1,$$

where f_{SDR} and f_{ML} are defined in (9), $c(\rho, \gamma)$ is

$$c(\rho, \gamma) = 1 + \frac{2(1 + \sqrt{\gamma})^2 \beta}{\gamma \rho^{\alpha-1}}, \quad (10)$$

and α, β are given by

$$\alpha = \begin{cases} 1/3, & \text{if } \gamma = 1, \\ 1/2, & \text{if } \gamma > 1; \end{cases} \quad \beta = \begin{cases} 4\sqrt[3]{4}, & \text{if } \gamma = 1, \\ 4\sqrt{\gamma}/\sqrt{\gamma-1}, & \text{if } \gamma > 1. \end{cases}$$

The value of the theorem can be easily seen if we compare the bound (10) with that of a random algorithm that simply generates a random vector $\mathbf{s}_{RND} \in \{-1, +1\}^n$ (independent of \mathbf{H}, \mathbf{v}) as an estimate of the solution. This random algorithm achieves the objective value $f_{RND} := \|\mathbf{y} - \sqrt{\rho} \mathbf{H} \mathbf{s}_{RND}\|^2$. Let $m, n \rightarrow \infty$ such that $m/n \rightarrow \gamma$ for some γ ($\gamma \geq 1$). It is straightforward to derive

$$\lim_{\substack{m, n \rightarrow \infty \\ m/n \rightarrow \gamma}} \frac{f_{RND}}{m} = (2\rho + 1). \quad (11)$$

A similar ratio for the ML detector has been bounded in [9]:

$$\lim_{\substack{m, n \rightarrow \infty \\ m/n \rightarrow \gamma}} P \left\{ \frac{1}{2} \leq \frac{f_{ML}}{m} \right\} = 1. \quad (12)$$

The expressions (11) and (12) lead to the conclusion that the random algorithm provides the approximation ratio $c(\rho, \gamma) = 4\rho + 2$ in probability, which is significantly worse than the bound (10).

In addition to the claim above, the SDR algorithm offers theoretical performance guarantees when ρ grows with problem size. Define the following random variable:

$$\mathcal{A}(n, m, \rho) := \frac{\|\mathbf{H}^\dagger \mathbf{v}\|_2}{\sqrt{\rho} \lambda_{\min}(\mathbf{H}^\dagger \mathbf{H})}. \quad (13)$$

It is shown in [9], [10] that the semidefinite relaxation (6) is tight (rank-1 solution matrix) when $\mathcal{A}(n, m, \rho) < 1$, and in that case the ML detection problem is solvable in polynomial time. The result below states the rate at which ρ needs to grow with $n, m \rightarrow \infty$ to ensure that the sufficient condition $\mathcal{A}(n, m, \rho) < 1$ holds with probability 1.

Theorem 2: Consider the random channel (1) and (2) specified with real or complex Rayleigh \mathbf{H} , i.e. $H_{ik} \sim \mathcal{N}(0, 1/n)$, or $H_{ik} \sim \mathcal{CN}(0, 1/n)$. Let

$$\rho = \begin{cases} \Omega(m), & \text{when } \gamma > 1, \\ \Omega(m^5 m^\epsilon), \forall \epsilon > 0, & \text{when } \gamma = 1. \end{cases}$$

Then, the semidefinite program (6) has a rank-1 solution:

$$P \left\{ \lim_{\substack{m, n \rightarrow \infty \\ m/n \rightarrow \gamma \geq 1}} \mathcal{A}(n, m, \rho) < 1 \right\} = 1.$$

C. Low-rank semidefinite relaxation (PSK detector)

A tighter (non-convex) semidefinite relaxation of the ML detection problem (4) for M -PSK constellations can empirically deliver superior performance in some scenarios, although thorough theoretical analysis of a non-convex formulation is substantially more complicated. The constraint $\mathbf{x} \in \mathcal{C}_{M\text{-PSK}}^{n+1}$ implies that each entry $x_i, i = 1, \dots, n+1$, of vector \mathbf{x} can take on values $\exp(j\phi_i)$, where $\phi_i = 2\pi i/M, \forall i = 1, \dots, M$. Unlike (6) we can relax only the constraint $\mathbf{x} \in \mathcal{C}_{M\text{-PSK}}^{n+1}$ in (4) to allow arbitrary phases ϕ_i of $x_i = \exp(j\phi_i), i = 1, \dots, n+1$, i.e. $|x_i| = 1, \forall i$. Since $\mathbf{X} = \mathbf{x}\mathbf{x}^\dagger$, the relaxed constraint can be written as $\text{diag}(\mathbf{X}) = \mathbf{e}$. An equivalent form of the rank-1 constraint $\mathbf{X} = \mathbf{x}\mathbf{x}^\dagger$ with implicit vector \mathbf{x} is $\{\text{rank}(\mathbf{X}) = 1, \mathbf{X} \succeq 0\}$. Thus, we obtain the following non-convex relaxation:

$$\begin{aligned} f_{LRR} := \min \quad & \text{Trace}(\mathbf{Q}\mathbf{X}) \\ \text{s.t.} \quad & \text{diag}(\mathbf{X}) = \mathbf{e}, \quad \mathbf{X} \succeq 0, \\ & \text{rank}(\mathbf{X}) = 1. \end{aligned} \quad (14)$$

Let \mathbf{x}_R and \mathbf{x}_I represent the real and imaginary parts of vector \mathbf{x} . For a real symmetric matrix \mathbf{Q} the objective function in (14) is:

$$\text{Trace}(\mathbf{Q}\mathbf{x}\mathbf{x}^\dagger) = \text{Trace}(\mathbf{Q}(\mathbf{x}_R\mathbf{x}_R^\dagger + \mathbf{x}_I\mathbf{x}_I^\dagger)) = \text{Trace}(\mathbf{Q}\mathbf{Z}),$$

where $\mathbf{Z} \triangleq \mathbf{x}_R\mathbf{x}_R^\dagger + \mathbf{x}_I\mathbf{x}_I^\dagger \succeq 0$. Therefore, the complex rank-1 constraint $\mathbf{X} = \mathbf{x}\mathbf{x}^\dagger$ is equivalent to the real constraints $\{\text{rank}(\mathbf{Z}) \leq 2, \mathbf{Z} \succeq 0\}$, thus the relaxation of the ML detection problem (3) with real matrix \mathbf{Q} is given by:

$$\begin{aligned} f_{LRR} := \min \quad & \text{Trace}(\mathbf{Q}\mathbf{Z}) \\ \text{s.t.} \quad & \text{diag}(\mathbf{Z}) = \mathbf{e}, \quad \mathbf{Z} \succeq 0, \\ & \text{rank}(\mathbf{Z}) \leq 2. \end{aligned} \quad (15)$$

In the context of combinatorial optimization which corresponds to the case of BPSK modulation, the above relaxation was first considered in [4] as a low-rank semidefinite relaxation of a Boolean quadratic maximization problem. From a digital communications standpoint, we are interested in this relaxation for general M -PSK signals with complex or real \mathbf{Q} . For a complex matrix \mathbf{Q} we can double dimensions of the problem and obtain a low-rank relaxation similar to (15).

In this work we use a different formulation when \mathbf{Q} is complex. In particular, define the following set:

$$\mathbb{U}^{n+1} \triangleq \{ \mathbf{x} \mid |x_i| = 1, \forall i = 1, \dots, n+1 \}.$$

The feasible set in (14) is equivalent to the set given by: $\{\mathbf{X} = \mathbf{x}\mathbf{x}^\dagger, \mathbf{x} \in \mathbb{U}^{n+1}\}$, hence, we can write (14) in the form

$$\min_{\mathbf{x} \in \mathbb{U}^{n+1}} \mathbf{x}^\dagger \mathbf{Q} \mathbf{x}. \quad (16)$$

The global phase ambiguity in \mathbf{x} is removed if the entries of vector \mathbf{x} are rotated by a common phase ϕ_0 to ensure that $x_{n+1} = 1$, i.e. $\mathbf{x} := \exp(j\phi_0)\mathbf{x}$, where $\phi_0 = -\phi_{n+1}$.

Despite the fact that the relaxed problem (16) is NP-hard [14], we have a theoretical bound on the quality of local minimizers. Let us formulate problem (16) in the homogeneous form:

$$\hat{\mathbf{z}} = \arg \min_{\mathbf{x} \in \mathbb{U}^{n+1}} \text{Trace}(\mathbf{Q}\mathbf{x}\mathbf{x}^\dagger)$$

where \mathbf{x}, \mathbf{Q} are defined in (5). Note that a vector $\mathbf{x}(\phi)$ in \mathbb{U}^{n+1} can be parameterized by an angular vector $\phi = (\phi_1, \dots, \phi_{n+1})^\dagger \in \mathbb{R}^{n+1}$, i.e., $x_i = e^{j\phi_i}, \forall i$. Thus, we have

$$(\mathbf{x}(\phi)\mathbf{x}(\phi)^\dagger)_{ik} = e^{j\phi_i}(e^{j\phi_k})^* = e^{j(\phi_i - \phi_k)}$$

Hence, the objective function in the minimization problem (16) is equivalent to

$$f(\phi) \triangleq \text{Trace}(\mathbf{Q}\mathbf{x}(\phi)\mathbf{x}(\phi)^\dagger), \quad \forall \phi \in \mathbb{R}^{n+1}. \quad (17)$$

Let $f_{\max} = \max_{\phi} f(\phi)$ and $f_{\min} = \min_{\phi} f(\phi)$ denote the global maximum and minimum values of the objective function (17). A vector $\hat{\phi}$ is called a δ -minimizer, $\delta \in [0, 1]$, if

$$\frac{f(\hat{\phi}) - f_{\min}}{f_{\max} - f_{\min}} \leq \delta.$$

When the above inequality holds, the function value $f(\hat{\phi})$ is called a δ -minimum. The theoretical bound on the quality of the local minima is given by the following theorem [13].

Theorem 3: *Every local minimizer $\hat{\phi}$ of (17) is a $\frac{1}{2}$ -minimizer and $f(\hat{\phi})$ is a $\frac{1}{2}$ -minimum of (17). If, in addition, $\mathbf{x}(\hat{\phi})$ is feasible for (4), then $\mathbf{x}(\hat{\phi})$ is a $\frac{1}{2}$ -maximizer for the ML detection problem.*

III. IMPLEMENTATION OF THE SDR DETECTOR

In this section, we present an efficient implementation for the detector based on semidefinite relaxation (6).

A. Dual-scaling interior-point method

The dual-scaling interior point method [2] has been developed to solve general large-scale semidefinite programs. In addition to the advantages associated with a standard interior point method (polynomial worst-case complexity, certificates of infeasibility when no solution exists, robustness and scalability), the dual-scaling method efficiently exploits the structure and sparsity in the dual semidefinite programs.

Existing implementations of the semidefinite relaxation detector rely on interior-point methods which solve the primal problem (6) and/or the following dual problem with variables $\mathbf{g} \in \mathbb{R}^{n+1}$:

$$\begin{aligned} f_{SDP} := \max \quad & \mathbf{g}^\dagger \mathbf{e} \\ \text{s.t.} \quad & \mathbf{Q} - \text{Diag}(\mathbf{g}) \succeq 0, \end{aligned} \quad (18)$$

where $\text{Diag}(\mathbf{g})$ denotes a diagonal matrix with diagonal entries equal to those of vector \mathbf{g} . For any $\nu > 0$ define $\{\mathbf{X}_\nu, \mathbf{g}_\nu, \mathbf{S}_\nu\}$ as the solution to

$$\begin{aligned} \text{diag}(\mathbf{X}_\nu) &= \mathbf{e}, \\ \mathbf{Q} - \text{Diag}(\mathbf{g}_\nu) &= \mathbf{S}_\nu, \\ \mathbf{S}_\nu \mathbf{X}_\nu &= \nu \mathbf{I}. \end{aligned} \quad (19)$$

As $\nu \rightarrow 0^+$ the sequence $\{\mathbf{X}_\nu, \mathbf{g}_\nu, \mathbf{S}_\nu\}$ of solutions of (19) forms a central path in the feasible region and converges to the optimal solution of (18). The dual-scaling algorithm generates iterates that approximately follow the central path. At each

step, the updating direction is calculated as the solution to the following linearization of (19):

$$\begin{aligned} \text{diag}(\Delta \mathbf{X}) &= \mathbf{0}, \\ \Delta \mathbf{S} + \text{Diag}(\Delta \mathbf{g}) &= \mathbf{0}, \\ \nu \mathbf{S}_\nu^{-1} \Delta \mathbf{S} \mathbf{S}_\nu^{-1} + \Delta \mathbf{X} &= \nu \mathbf{S}_\nu^{-1} - \mathbf{X}_\nu. \end{aligned}$$

Solving this system of matrix equations in terms of dual variables $\Delta \mathbf{g}$, we obtain the following condition:

$$\nu (\mathbf{S}_\nu^{-1} \circ \mathbf{S}_\nu^{-1}) \Delta \mathbf{g} = \mathbf{e} - \nu \text{diag}(\mathbf{S}_\nu^{-1}), \quad (20)$$

where \circ denotes Hadamard (component-wise) product.

After computing $\Delta \mathbf{g}$ from (20), an inexact line search $\mathbf{g}^+ := \mathbf{g}_\nu + \tau \Delta \mathbf{g}$ is performed where step size τ is obtained by minimizing the dual potential function

$$f^d := \gamma \log(\bar{z} - (\mathbf{g}^+)^{\dagger} \mathbf{e}) - \log \det(\mathbf{Q} - \text{Diag}(\mathbf{g}^+)),$$

where $\bar{z} = \text{Trace}(\mathbf{Q}\mathbf{X})$ is an upper bound computed at some primal feasible \mathbf{X} . The algorithm starts with $\tau := \min\{1, 0.95\tau_{max}\}$ and then backtracks until sufficient descent or termination tolerance is achieved. The maximum feasible step size τ_{max} that ensures feasibility of $\mathbf{g}^+ \in \{\mathbf{g} | \mathbf{Q} - \text{Diag}(\mathbf{g}) \succeq \mathbf{0}\}$, is given by the distance to the boundary of the semidefinite cone, $\lambda_{max}^{-1}(\mathbf{L}^{-1} \text{Diag}(\Delta \mathbf{g})(\mathbf{L}^{-1})^{\dagger})$, where \mathbf{L} is the lower triangular Cholesky factor of $\mathbf{S}_\nu = \mathbf{Q} - \text{Diag}(\mathbf{g}_\nu)$. To compute the largest eigenvalue of $\mathbf{A} \triangleq \mathbf{L}^{-1} \text{Diag}(\Delta \mathbf{g})(\mathbf{L}^{-1})^{\dagger}$ we apply Lanczos procedure [25]. Starting from a vector \mathbf{u}_1 , $\|\mathbf{u}_1\| = 1$, Lanczos procedure iteratively constructs a basis $\mathbf{U}_i = [\mathbf{u}_1, \dots, \mathbf{u}_i]$ in the Krylov subspace $\{\mathbf{u}_1, \mathbf{A}\mathbf{u}_1, \dots, \mathbf{A}^{i-1}\mathbf{u}_1\}$, and a tridiagonal matrix \mathbf{T}_i , $i \times i$, such that

$$\mathbf{A}\mathbf{U}_i = \mathbf{U}_i \mathbf{T}_i + t_{i+1} \mathbf{u}_{i+1} \mathbf{e}_i^{\dagger}, \quad \mathbf{U}_i^{\dagger} \mathbf{A} \mathbf{U}_i = \mathbf{T}_i,$$

where \mathbf{e}_i is the i -th basis vector. The extreme eigenvalues of \mathbf{A} are usually well approximated by those of \mathbf{T}_i with far fewer iterations than n .

B. Warm start with the truncated sphere decoder

The sphere decoder with adjustable radius search serves as a fast heuristic test of low noise channel realizations. The initialization routine of the SDR detector uses a truncated version of the sphere decoder [26] (see Figure 2) to restrict its exponential complexity with the following constant parameters: initial radius R_0 , radius step size ΔR , upper bound N_r on the number of radius increases, and upper bound N_v on the number of objective function computations.

The maximum number of sphere expansions is selected to ensure that the complexity of the truncated sphere decoder C(SD) does not dominate the complexity of the dual-scaling algorithm C(SDP):

$$\mathcal{O}(n^{3.5}) \simeq \text{C(SDP)} \simeq \text{C(SD)} \simeq \mathcal{O}\left((N_r \Delta R)^{n/\rho}/\rho\right).$$

Thus, the number of times the algorithm is allowed to increase the radius of the sphere is set $N_r = \mathcal{O}\left((n^{3.5} \rho)^{\rho/n} / \Delta R\right)$. For the heuristic radius search procedure the expected number of vectors found within a sphere is exponential, $2^{n/\rho}$. The SDR detector heuristically sets the number of vectors allowed

Input: $R_0, \Delta R, N_r, N_v$

- R_0 is starting radius
- ΔR is radius step size
- N_r is number of radii to be searched
- N_v is number of vectors to be searched

1. $R := R_0$
2. **while** (number of radii searched $\leq N_r$)
3. **if** (found a vector inside sphere with radius R)
4. $\mathbf{s}_{min} := \mathbf{e}; f_{min} := \|\mathbf{y} - \sqrt{\rho} \mathbf{H}\mathbf{e}\|^2$
5. **while** (number of vectors searched $\leq N_v$)
6. **for each** (\mathbf{s} found in the sphere)
7. $f(\mathbf{s}) := \|\mathbf{y} - \sqrt{\rho} \mathbf{H}\mathbf{s}\|^2$
8. **if** ($f(\mathbf{s}) < f_{min}$)
9. $f_{min} := f(\mathbf{s}); \mathbf{s}_{min} = \mathbf{s}$
10. **end if**
11. **end for**
12. **if** (no vectors in sphere with radius R)
13. **return** ML solution \mathbf{s}_{min}
14. **end if**
15. **end while**
16. **return** best guess \mathbf{s}_{min}
17. **end if**
18. $R := R + \Delta R$
19. **end while**
20. **return** \mathbf{s}_{min} is not found

Fig. 2. Truncated version of the sphere decoder

to be searched in a sphere to be a decreasing function of ρ and n : $N_v = \max\{2, \mathcal{O}(2^{-n/\rho}/\rho)\}$.

The smallest objective value f_{min} achieved by the truncated sphere decoder is used to initialize upper bound $\bar{z} := f_{min}$ in the dual-scaling algorithm. In our experience, a good initial upper bound improves the convergence of the dual-scaling interior-point method.

C. Dimension reduction technique

Instead of using a standard randomized rounding procedure [16] after solving SDP (6), we introduce a dynamic dimension reduction technique which allows us to round symbols at intermediate steps of the dual-scaling algorithm. After a constant number of steps of the dual-scaling algorithm, we use Lanczos procedure to compute the principal eigenvector \mathbf{v}^{max} of \mathbf{X}_ν in (19) to check if there is a strong bias in distribution (7) for some bits. Given a constant parameter $\sigma, 0 < \sigma < 1$, the dynamic dimension reduction strategy rounds the bits with $|\text{Re}\{v_i^{max}\}| > \sigma \max_i |\text{Re}\{v_i^{max}\}|$, and subsequently reduces the problem size and complexity of solving (19), see Figure 3.

The principal eigenvector \mathbf{v}^{max} of \mathbf{X}_ν can be computed without expensive computation of primal \mathbf{X}_ν . Equations (19) show that the eigenvectors of \mathbf{X}_ν and \mathbf{S}_ν are the same on the central path, and eigenvector \mathbf{v}^{max} of \mathbf{X}_ν is equal to the eigenvector of \mathbf{S}_ν corresponding to the smallest eigenvalue:

$$\mathbf{v}^{max} = \arg \min_{\mathbf{u}, \|\mathbf{u}\|=1} \mathbf{u}^{\dagger} \mathbf{S}_\nu \mathbf{u} = \arg \min_{\mathbf{u}, \|\mathbf{u}\|=1} \mathbf{u}^{\dagger} (\mathbf{Q} - \text{Diag}(\mathbf{g}_\nu)) \mathbf{u}.$$

After rounding at each iteration, a new matrix \mathbf{Q} with reduced dimensions can be updated recursively in order $\mathcal{O}(n^2)$

```

Input:  $\sigma, S_{rnd}$ 
    •  $\sigma, 0 < \sigma < 1$  is reliability threshold
    •  $S_{rnd}$  is set of rounded symbols
// Find the most reliable symbol
1.  $S_{rnd} := \emptyset; w_{max} := |\text{Re}\{v_1^{max}\}|; i_{max} := 1$ 
2. for ( $\forall i, 1 < i \leq n$ )
3.   if ( $|\text{Re}\{v_i^{max}\}| > w_{max}$ )
4.      $w_{max} := |\text{Re}\{v_i^{max}\}|; i_{max} := i$ 
5.   end if
6. end for
// Round symbols  $\sigma$ -fraction away from  $w_{max}$ 
7. for ( $\forall i, 1 \leq i \leq n$ )
8.   if ( $|\text{Re}\{v_i^{max}\}| > \sigma w_{max}$ )
9.     // Round the  $i$ -th symbol
10.     $x_i := \text{sign}(\text{Re}\{v_i^{max}(v_{n+1}^{max})^*\})$ 
11.     $S_{rnd} := \{S_{rnd}, i\}$ 
12.   end if
13. end for
// Reduce problem dimension
14.  $n := n - |S_{rnd}|$ 
15. Recursively update matrix  $\mathbf{Q}$ 
    
```

Fig. 3. Dimension reduction technique

operations. Given the set of rounded bits S_{rnd} we remove columns $\mathbf{h}_i, i \in S_{rnd}$ of matrix \mathbf{H} and update the received vector $\mathbf{y} := \mathbf{y} - \sum_{i \in S_{rnd}} x_i \mathbf{h}_i$. Matrix \mathbf{Q} can be similarly updated by removing the i -th rows and columns for $i \in S_{rnd}$, and recomputing the last row and column with updated values of $-\sqrt{\rho} \mathbf{H}^\dagger \mathbf{y}$, and $\mathbf{y}^\dagger \mathbf{y}$.

D. Complexity

Due to truncation of the sphere decoder in the warm start procedure, the complexity of the SDR detector is dominated by complexity of the dual-scaling algorithm, $\mathcal{O}(n^{3.5})$. The complexity of the dimension reduction technique, $\mathcal{O}(n^2 m)$, is dominated by Lanczos procedure to compute the principal eigenvector \mathbf{v}^{max} .

IV. IMPLEMENTATION OF THE PSK DETECTOR

In this section, we present an efficient implementation for the detector based on the low-rank semidefinite relaxation (16).

A. Warm start with unconstrained minimization

We propose the following initialization method: a good starting point can be obtained with a fixed number of projected coordinate descent iterations for the relaxed problem given by

$$\begin{aligned}
 \min_{x_k} \quad & f(\mathbf{x}) = \mathbf{x}^\dagger \mathbf{Q} \mathbf{x} \\
 \text{s.t.} \quad & |x_k| \leq 1 + \zeta, \quad k = 1, \dots, n, \\
 & x_{n+1} = 1,
 \end{aligned}$$

where \mathbf{x} and \mathbf{Q} are defined in (5), $\zeta > 0$ is a parameter, and $\zeta \rightarrow 0$ with iteration number. Specifically, at each iteration we take a step proportional to $-\frac{\partial f(\mathbf{x})}{\partial x_k}$ for some $k \in \{1, \dots, n\}$, and project it onto the set $\{\mathbf{x} \in \mathbb{C}^n \mid |x_k| \leq 1 + \zeta, x_{n+1} = 1\}$.

B. Dimension reduction technique

Let $S_{rnd} \subset \{1, \dots, n\}$ denote the set of indices of rounded symbols $x_k, k = 1, \dots, n$. Initially, we have $S_{rnd} = \emptyset$. The core of the PSK detector is the projected coordinate descent method that solves the following problem with a dynamically adjusted parameter $\omega > 0$:

$$\begin{aligned}
 \min_{x_k} \quad & f(\mathbf{x}) = \mathbf{x}^\dagger \mathbf{Q} \mathbf{x} \\
 \text{s.t.} \quad & (1 + \omega)^{-1} \leq |x_k| \leq 1 + \omega, \quad \forall k \notin S_{rnd}, \\
 & x_{n+1} = 1.
 \end{aligned} \tag{21}$$

Parameter ω (which is set in the algorithm to decrease linearly to 0) allows a continuous homotopy of the feasible region to the unit circle. An additional, linearly increasing parameter θ is used to implement the dimension reduction technique. The k -th entry x_k is rounded to the closest constellation point prior to algorithm termination if it falls in the set:

$$\{x_k \mid \text{distance}(\phi(x_k), \mathcal{C}_{M\text{-PSK}}) \leq \theta/2\},$$

where $\phi(x_k)$ denotes the phase of the complex value x_k . The early rounding of entries of \mathbf{x} reduces problem size and improves algorithm efficiency. When x_k is rounded, we update the set of rounded entries to include the k -th index, $S_{rnd} := \{S_{rnd}, k\}$, in the subsequent iterations of (21). Parameters ω and θ are updated after minimization is performed along all non-rounded entries of \mathbf{x} , see Figure 4. After the last iteration, each remaining entry of \mathbf{x} is rounded to the closest M -PSK symbols.

C. Complexity

The coordinate descent method requires the computation of the objective function and its gradient. The complexity of the initialization phase is cubic due to the cost of computing matrix \mathbf{Q} . However, such computation is performed only once and is common in other quasi-ML strategies (compare with the cost of QR-factorization of matrix \mathbf{H} to compute the zero-forcing estimate in the sphere decoder).

In subsequent iterations, the objective function and its partial derivative are updated recursively along each coordinate direction in linear time. Notice that an entry x_k affects only $2n - 1$ terms in the quadratic form $f(\mathbf{x}) = \mathbf{x}^\dagger \mathbf{Q} \mathbf{x}$. Reusing the value of the objective function and its gradient vector from the previous iteration and recomputing the contribution of the new k -th component to $f(\mathbf{x})$ and $\frac{\partial f(\mathbf{x})}{\partial x_k}$ can be done with linear complexity. Complexity of the dimension reduction procedure is also linear since it modifies only one entry at a time. The coordinate descent method runs for a fixed number of iterations over all entries of \mathbf{x} , therefore, the complexity of the coordinate descent algorithm (warm start and the dimension reduction technique) is $\mathcal{O}(k^2)$, where $k = \max\{m, n\}$.

V. SIMULATIONS

A. Simulation setup

In this section we present Monte Carlo simulations of the following detectors: (1) sphere decoder [1], [21]; (2) SDR detector; (3) SDR detector without warm start; (4) PSK detector; (5) SDP detector [16], based on SeDuMi [23]. We will

```

Input:  $\mathbf{Q}, \zeta_0, \omega_0, n_1, n_2$ 

- $n_1$  is the number of iterations for warm start
- $n_2$  is the number of dimension reduction iterations
- $\zeta_0, \omega_0$  are parameters of feasible region homotopy

// Warm Start:

1. for ( $\forall i, 1 \leq i \leq n_1$ )
2.  $\zeta := \zeta_0(n_1 - i)/(n_1 - 1)$
3. for ( $\forall k, 1 \leq k \leq n$ )
4.  $\min_{x_k} f(\mathbf{x}), \quad \text{s.t. } |x_k| \leq 1 + \zeta;$
5. end for
6. end for

// Dimension Reduction:

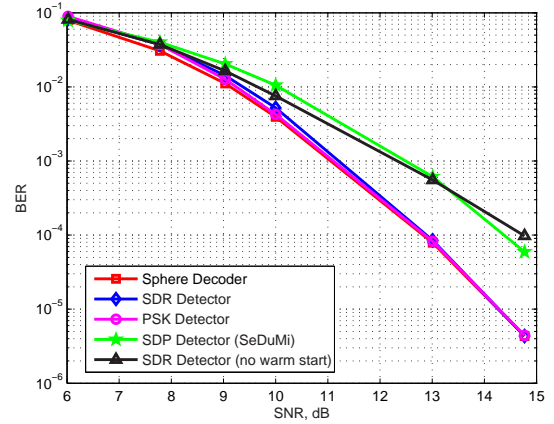
7.  $S_{rnd} := \emptyset$  // The set of rounded entries is empty
8. for ( $\forall i, 1 \leq i \leq n_2$ )
9.  $\omega := \omega_0(n_2 - i)/(n_2 - 1)$
10.  $\theta := 2\pi(i - 1)/(M(n_2 - 1))$
11. for ( $\forall k$  s.t.  $k \notin S_{rnd}$ )
12. if ( $\exists p_j \in \mathcal{C}_{M\text{-PSK}}$  s.t.  $|\phi(x_k) - \phi(p_j)| \leq \theta/2$ )
13.  $x_k := p_j$  // Round the entry
14.  $S_{rnd} := \{S_{rnd}, k\}$  // Add index k to S_rnd
15. if ( $|S_{rnd}| == n$ ) // If all x_k are rounded
16. return solution  $\mathbf{x}$
17. end if
18. else
19.  $\min_{x_k} f(\mathbf{x}), \quad \text{s.t. } (1 + \omega)^{-1} \leq |x_k| \leq 1 + \omega;$
20. end if
21. end for
22. end for
23. return solution  $\mathbf{x}$

```

Fig. 4. PSK detector algorithm

focus on 3 performance metrics, namely BER performance, average and worst-case running time (measured in seconds, CPU: AMD Athlon 64, 3000+).

We have selected the Schnorr-Euchner variant of the sphere decoder [1], [21] as a benchmark due to its excellent performance for small-to-medium size problems and the availability of codes (courtesy of Prof. G.B. Giannakis, University of Minnesota). **The performance comparison of semidefinite relaxation and tree search strategies [19] in the context of the coded communication system suggests that intelligently designed semidefinite relaxation detectors can outperform tree search detectors [20].** Various other quasi-ML detectors are either not available in the ready-to-use form, significantly more complex, or exhibit significant BER degradation as compared to the true ML detector. Following [22] and to make the comparison fair, we do not rely on an ad-hoc method [6] to tune the input radius for the sphere decoder based on system parameters. Instead, we have set the infinite radius in the Schnorr-Euchner variant of the sphere decoder to ensure that we obtain the optimal solution and have ML-like BER performance. The SDP detector is implemented with SeDuMi optimization toolbox [23] for Matlab, and the other detectors are implemented in ANSI C with mex interfaces for Matlab. In our implementation of the SDR detector we used DSDP5 software package [3] that contains an efficient implementation


 Fig. 5. BER performance, $n = m = 20$, QPSK.

of the dual-scaling algorithm. The implementations of the SDR and PSK detectors described in this paper are available online [29] for further comparison. For high-order constellations (e.g. 16-QAM, 8-PSK), the gray-code mapping of bits onto complex symbols is used to compute BER. Our results show that, among all the detectors tested, no single one performs uniformly the best for all simulated channels.

1) *A. Complex communication channel:* Maximum-likelihood detection (3) can be generalized to complex fading channels. Define the real and imaginary parts of channel matrix $\mathbf{H} = \mathbf{H}_R + j\mathbf{H}_I$, noise $\mathbf{v} = \mathbf{v}_R + j\mathbf{v}_I$, transmitted signals $\mathbf{s} = \mathbf{s}_R + j\mathbf{s}_I$ and vector of received signals $\mathbf{y} = \mathbf{y}_R + j\mathbf{y}_I$. Then, the complex channel model (1) is equivalent to the following real valued channel with the double dimension:

$$\begin{bmatrix} \mathbf{y}_R \\ \mathbf{y}_I \end{bmatrix} = \sqrt{\rho} \begin{bmatrix} \mathbf{H}_R & -\mathbf{H}_I \\ \mathbf{H}_I & \mathbf{H}_R \end{bmatrix} \begin{bmatrix} \mathbf{s}_R \\ \mathbf{s}_I \end{bmatrix} + \begin{bmatrix} \mathbf{v}_R \\ \mathbf{v}_I \end{bmatrix}.$$

Running the SDR or PSK detector with equivalent channel matrix \mathbf{H}_{eq} and received signals \mathbf{y}_{eq}

$$\mathbf{H}_{eq} = \begin{bmatrix} \mathbf{H}_R & -\mathbf{H}_I \\ \mathbf{H}_I & \mathbf{H}_R \end{bmatrix}, \quad \mathbf{y}_{eq} = \begin{bmatrix} \mathbf{y}_R \\ \mathbf{y}_I \end{bmatrix},$$

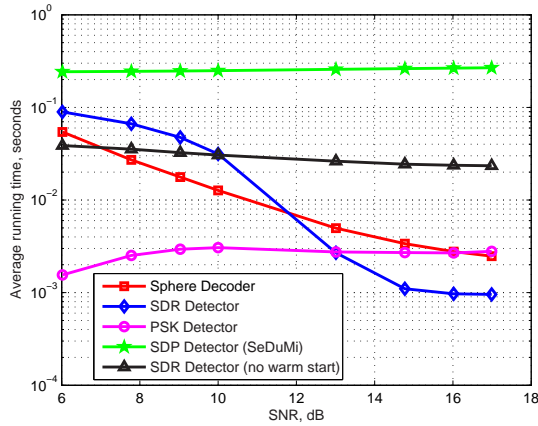
we obtain quasi-ML estimates of \mathbf{s}_R and \mathbf{s}_I which can be combined to reconstruct the complex estimate of transmitted signals $\mathbf{s} = \mathbf{s}_R + j\mathbf{s}_I$.

2) *PAM constellations:* A signal drawn from a uniform 2^M -PAM constellation can be represented as a linear combination of M binary signals:

$$s_k = \frac{1}{\mu_1} \sum_{i=0}^{M-1} b_{ki} 2^i = \frac{1}{\mu_1} \mathbf{b}_k^\dagger \mathbf{c}, \quad \mathbf{b}_k \in \{-1, +1\}^M,$$

where vector $\mathbf{c} = [2^0, 2^1, \dots, 2^{M-1}]^\dagger$ specifies the 2^M -PAM constellation, normalization factor $\mu_1 \triangleq \sqrt{(4^M - 1)/3}$ is introduced to satisfy $E\{|s_k|^2\} = 1$, and \mathbf{b}_k contains the bit representation of signal s_k . A vector $\mathbf{s} \in \mathcal{C}_{2^M\text{-PAM}}^n$ of n signals drawn from 2^M -PAM constellation can be represented in terms of the corresponding matrix of bits:

$$\mathbf{s} = \frac{1}{\mu_1} \bar{\mathbf{B}} \mathbf{c}, \quad \bar{\mathbf{B}} = [\mathbf{b}_1, \dots, \mathbf{b}_n]^\dagger \in \{-1, +1\}^{n \times M}. \quad (22)$$


 Fig. 6. Average running time, $n = m = 20$, QPSK.

Thus, communication channel (1) can be written as follows

$$\mathbf{y} = (\sqrt{\rho}/\mu_1) \mathbf{H}\bar{\mathbf{B}}\mathbf{c} + \mathbf{v}.$$

Let $\text{vec}(\cdot)$ denote the operator that stacks a matrix into a vector column-by-column, and let \otimes denote Kronecker product. Applying $\text{vec}(\cdot)$ operator to the above equation results in

$$\mathbf{y} = (\sqrt{\rho}/\mu_1) \mathbf{H}_{eq}\mathbf{b} + \mathbf{v}, \quad \mathbf{H}_{eq} \triangleq \mathbf{c}^\dagger \otimes \mathbf{H} \quad (23)$$

where signal detection is performed over binary vector $\mathbf{b} = \text{vec}(\bar{\mathbf{B}}) \in \{-1, +1\}^{nM}$. The SDR or PSK detector can be applied to efficiently solve (23) followed by reconstruction (22) of the original PAM-modulated signals.

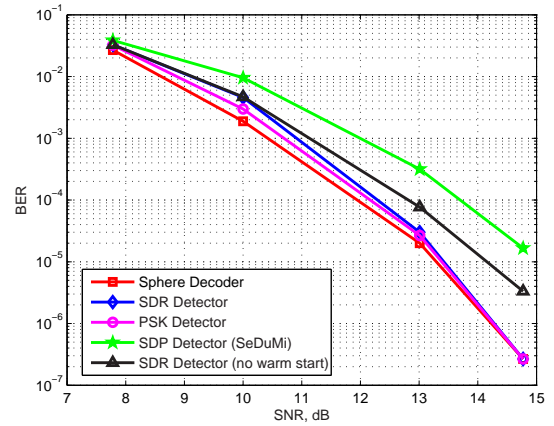
3) *PSK and QAM constellations*: Various strategies based on semidefinite relaxation have been proposed for general QAM constellations, e.g. [5], [17], [18], [22], [27], [28], and general PSK constellations [15]. These strategies offer different optimality on the complexity-performance tradeoff curve.

We solve the ML detection problem (3) over higher order PSK constellations with the PSK detector. We also investigate performance of both SDR and PSK detectors on channels with 16-QAM constellation. For this purpose, we apply a standard transformation of the transmitted signals drawn from higher order QAM constellations, 2^{2N} -QAM (e.g. 16-QAM, 64-QAM, etc.), to an equivalent channel with BPSK or QPSK constellation.

The SDR detector can be applied after sequential transformation of 2^{2N} -QAM signals in a complex channel to 2^N -PAM signals in the equivalent real channel followed by transformation to the equivalent channel with BPSK-modulated signals. An alternative transformation can be used to map 2^{2N} -QAM signals to QPSK signals. Specifically, a signal s_k drawn from 2^{2N} -QAM constellation can be written as

$$s_k = \frac{\sqrt{2}}{\mu_2} \sum_{i=0}^{M-1} p_{ki} 2^i = \frac{\sqrt{2}}{\mu_2} \mathbf{p}_k^\dagger \mathbf{c}, \quad \mathbf{p}_k \in C_{\text{QPSK}}^M,$$

where vector $\mathbf{c} = [2^0, 2^1, \dots, 2^{M-1}]^\dagger$ specifies the 2^{2M} -QAM constellation and normalization factor $\mu_2 \triangleq \sqrt{2(4^M - 1)}/3$ is selected to satisfy $E\{|s_k|^2\} = 1$. By analogy with the


 Fig. 7. BER performance, $n = m = 60$, BPSK.

transformation in the previous section, a vector $\mathbf{s} \in C_{2^{2M}\text{-QAM}}^n$ of n signals drawn from 2^{2M} -QAM constellation is given by:

$$\mathbf{s} = \frac{\sqrt{2}}{\mu_2} \bar{\mathbf{P}}\mathbf{c}, \quad \bar{\mathbf{P}} = [\mathbf{p}_1, \dots, \mathbf{p}_n]^\dagger \in C_{\text{QPSK}}^{n \times M}. \quad (24)$$

Substituting this equation into the communication channel model (1) and applying $\text{vec}(\cdot)$ operator, we arrive at the equivalent channel over QPSK-modulated signals:

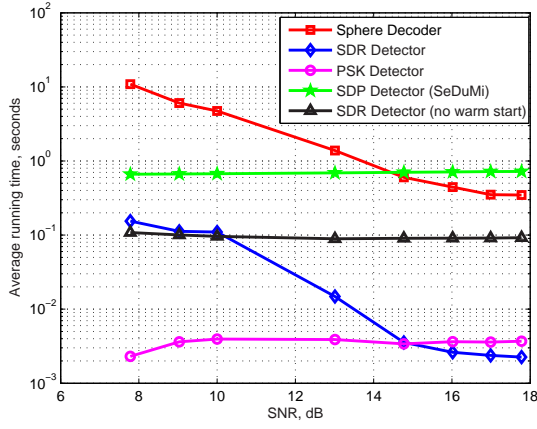
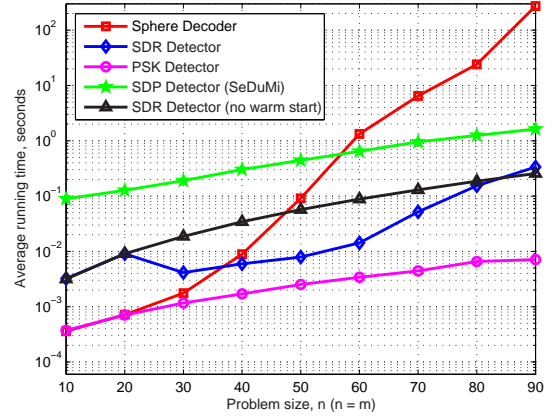
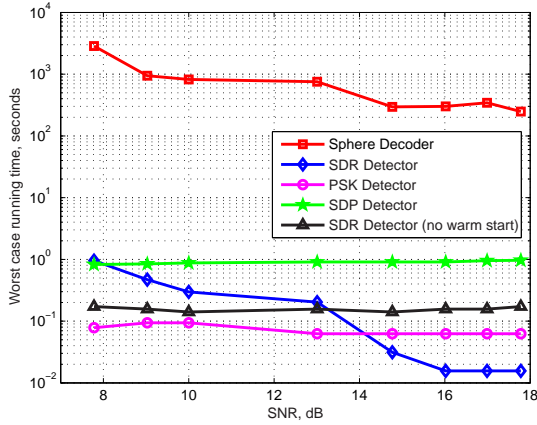
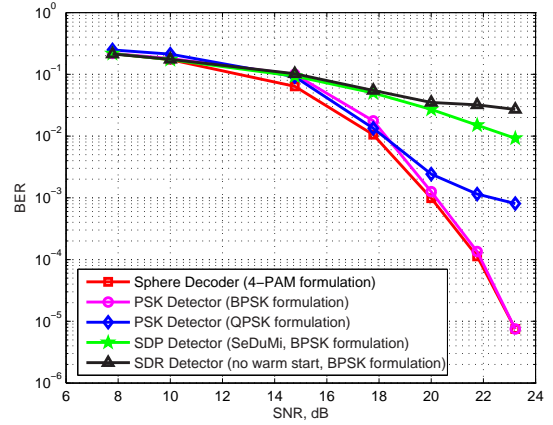
$$\mathbf{y} = (\sqrt{2\rho}/\mu_2) \mathbf{H}_{eq}\mathbf{p} + \mathbf{v}, \quad \mathbf{H}_{eq} \triangleq \mathbf{c}^\dagger \otimes \mathbf{H}, \quad (25)$$

where signal detection is performed over vector $\mathbf{p} = \text{vec}(\bar{\mathbf{P}}) \in C_{\text{QPSK}}^{nM}$. The PSK detector can be used to efficiently solve (25) followed by reconstruction of the QAM-modulated ML estimate, given by (24).

B. Simulation results

1) *Medium problem size with QPSK constellation*: BER performance and average running time of various detectors are shown in Figures 5 and 6 for a simulated scenario with $n = m = 20$, and QPSK constellation. Both SDR and PSK detectors closely follow the BER performance of the ML detector in all SNR regions. The SDP detector based on SeDuMi and the SDR detector without warm start exhibit a gap in BER performance of 1 – 2 dB in high SNR region. In low SNR region, the PSK detector offers an order of magnitude average speed improvement compared to other detectors, whereas in high SNR region, the sphere decoder, the SDR and PSK detectors achieve similar average running times, superior to the SeDuMi-based detector and the SDR detector without warm start.

2) *Large problem sizes*: Figures 7, 8, and 9 demonstrate BER performance, average and worst-case running time of the tested detectors for a large system ($m = n = 60$). The sphere decoder, the SDR and PSK detectors exhibit BER which is within 1 dB away from BER of ML detector, however the sphere decoder runs several orders slower than the SDR and PSK detectors for any SNR. Figures 8 and 9 show that for large systems both average and worst-case running time of the PSK detector (SDR detector) are superior in low (high) SNR region.


 Fig. 8. Average running time, $n = m = 60$, BPSK.

 Fig. 10. Average running time, $n = m$, $\rho = 13$ dB, BPSK.

 Fig. 9. Worst-case running time, $n = m = 60$, BPSK.

 Fig. 11. BER performance, $n = m = 10$, 16-QAM.

All polynomial complexity detectors enjoy highly predictable running time with small variance around its mean value.

We also compare the performance of these detectors as a function of problem size. Monte Carlo simulations of BER performance for a square communication channel with BPSK modulation and $\rho = 13$ dB are shown in Figure 10. We can see that the average running time of polynomial complexity detectors scales significantly better than exponentially growing average running time of the sphere decoder [11]. The PSK detector enjoys superior running time for all problem sizes. The warm start procedure implemented in the SDR detector delivers up to 10-times speed improvement for problem sizes 20–80 (compared to the SDR detector without SNR sensitive improvements).

3) *High order constellations*: For comparison purposes we select a communication system with $n = m = 10$, and 16-QAM modulation. At the receiver side we perform the following conversions to an equivalent channel that can be handled by the detectors:

- **sphere decoder (4-PAM formulation)**: channel $\mathbf{H} \in \mathbb{C}^{n \times n}$ and signals $\mathbf{s} \in \mathcal{C}_{16\text{-QAM}}^n$ are converted into $\mathbf{H}_{eq} \in \mathbb{R}^{2n \times 2n}$ and $\mathbf{s}_{eq} \in \mathcal{C}_{4\text{-PAM}}^{2n}$.
- **PSK detector (BPSK formulation)**: channel $\mathbf{H} \in \mathbb{C}^{n \times n}$

and signals $\mathbf{s} \in \mathcal{C}_{16\text{-QAM}}^n$ are converted into $\mathbf{H}_{eq} \in \mathbb{R}^{2n \times 4n}$ and $\mathbf{s}_{eq} \in \{-1, +1\}^{4n}$.

- **PSK detector (QPSK formulation)**: channel $\mathbf{H} \in \mathbb{C}^{n \times n}$ and signals $\mathbf{s} \in \mathcal{C}_{16\text{-QAM}}^n$ are converted into $\mathbf{H}_{eq} \in \mathbb{R}^{n \times 2n}$ and $\mathbf{s}_{eq} \in \mathcal{C}_{\text{QPSK}}^{2n}$.
- **SDP detector (BPSK formulation)**: channel $\mathbf{H} \in \mathbb{C}^{n \times n}$ and signals $\mathbf{s} \in \mathcal{C}_{16\text{-QAM}}^n$ are converted into $\mathbf{H}_{eq} \in \mathbb{R}^{2n \times 4n}$ and $\mathbf{s}_{eq} \in \{-1, +1\}^{4n}$.
- **SDR detector (without warm start, BPSK formulation)**: channel $\mathbf{H} \in \mathbb{C}^{n \times n}$ and signals $\mathbf{s} \in \mathcal{C}_{16\text{-QAM}}^n$ are converted into $\mathbf{H}_{eq} \in \mathbb{R}^{2n \times 4n}$ and $\mathbf{s}_{eq} \in \{-1, +1\}^{4n}$.

The performance metrics (i.e. BER, average and worst-case running time) for the quasi-ML detectors are presented in Figures 11, 12 and 13 respectively.

In these simulations, the SDR detector bypasses the warm start procedure because the channel matrix in the equivalent channel is fat, $2n \times 4n$. The PSK detector on the equivalent channel with BPSK modulation shows near-ML BER, however on the equivalent channel with QPSK modulation we can see BER degradation of several dB in high SNR region. The difference can be attributed to the global-minimum property of low-rank relaxation (see Remark after the proof of Theorem 5). The BER of the SDR and SDP detectors indicates significant

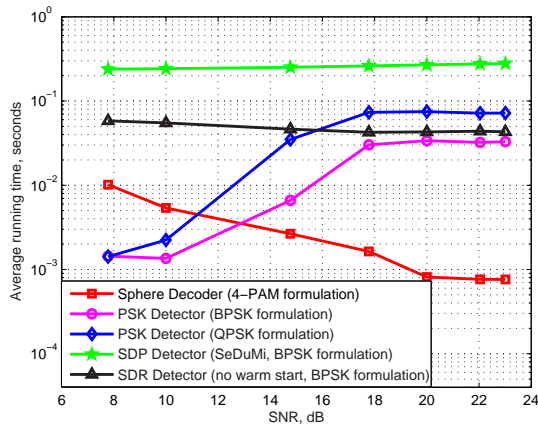


Fig. 12. Average running time, $n = m = 10$, 16-QAM.

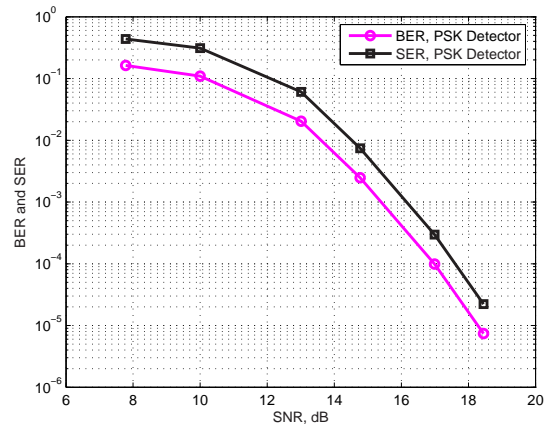


Fig. 14. BER and SER of the PSK detector, $n = m = 40$, 8-PSK.

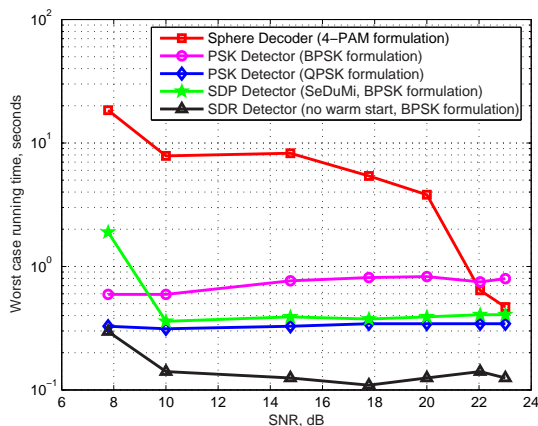


Fig. 13. Worst-case running time, $n = m = 10$, 16-QAM.

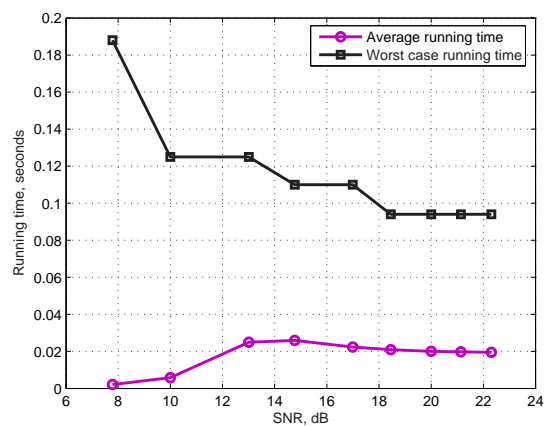


Fig. 15. Running time of the PSK detector, $n = m = 40$, 8-PSK.

loss in performance.

From the perspective of the average running time, the sphere decoder (PSK detector) is the fastest detector in high (low) SNR region (Figure 12). However, in applications limited by the worst-case latency, the SDR detector offers the best speed (Figure 13), while the sphere decoder suffers from long delays on bad channel/noise realizations and runs slower than all other detectors that we consider here. The worst-case running time of the polynomial complexity detectors is empirically immune to changes in SNR.

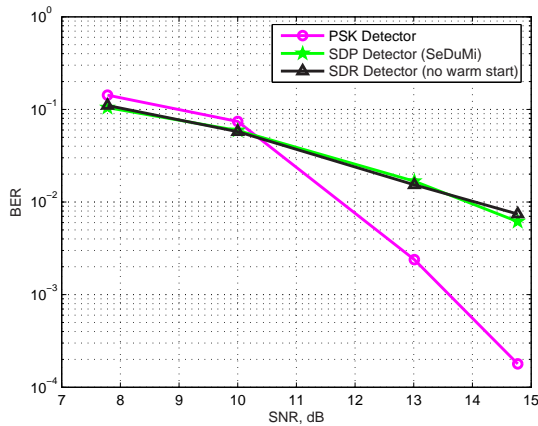
For a higher order M -PSK constellations ($M > 4$), the only practically viable strategy is based on the PSK detector. BER and SER for a communication system with $n = m = 40$, and 8-PSK constellation are shown in Figure 14. The average and worst-case running times of the PSK detector for the system are shown in Figure 15. We can see that the average running time of the PSK detector for this system does not exceed 30 msec, while the detection with the ML detector (exhaustive search) can not be performed for such system within any reasonable time.

4) *Fat channel matrices*: Quasi-ML detection strategies based on the PSK detector, SDR detector and SDP detector (SeDuMi) can be applied to communication channels with fat

channel matrices, i.e. $n > m$. Figures 16 and 17 present BER performance and running time of the above three detectors for a communication system with $n = 20$, $m = 15$ and QPSK-modulated signals. We can see that the PSK detector offers the best BER performance with the smallest average running time. The worst-case running time of the PSK detector exhibits a similar advantage.

Overall, we can draw the following conclusions from the presented results:

- The SDR and PSK detectors offer near-ML BER performance with the running time that is superior to that of other quasi-ML detectors on BPSK and QPSK constellations. The sphere decoder matches the running time of the semidefinite relaxation detectors on small systems at high SNR.
- The SDR and PSK detectors can be applied to detection of 16-QAM signals. The PSK detector with BPSK transformation of the channel delivers near-ML BER and impressive running time in low SNR region (less than 10 dB). For the systems with 16-QAM modulation operating at higher SNR, the sphere decoder and alternative semidefinite strategies [5], [17], [18], [22], [27], [28] offer better BER performance or running time.


 Fig. 16. BER performance, $n = 20$, $m = 15$, QPSK.

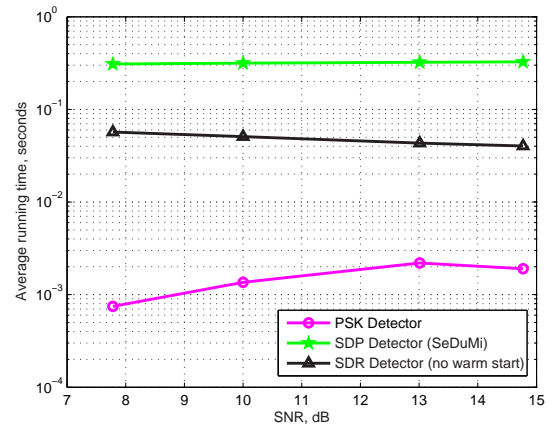
- The SDR detector is superior to the SeDuMi-based implementation of the semidefinite relaxation detector [16] both in the BER performance and the running time. The dynamic dimension reduction strategy allows the SDR detector to make decisions on the most reliable bits first, thus improving the BER performance. By eliminating the rounded bits the SDR detector reduces the problem size, rendering subsequent interior point iterations cheaper, thereby improving the running time. In addition, the dual scaling algorithm at the core of the SDR detector is faster than the SeDuMi implementation of the interior point method.

VI. CONCLUSIONS

The ML detection problem is central in digital communications and is known to be NP-hard. The paper presents **two efficient** approaches based on semidefinite relaxations of the ML detection problem. For both QAM and M -PSK constellations we develop approximation algorithms that can empirically deliver near optimal BER performance with a worst-case polynomial complexity. Numerical simulations of BER performance and running time indicate that the presented detectors can outperform or match BER performance and running time of the popular sphere decoder and the SeDuMi-based SDP detector.

REFERENCES

- [1] E. Agrell, T. Eriksson, A. Vardy, and K. Zeger, "Closest point search in lattices," *IEEE Transactions on Information Theory*, vol. 48, pp. 2201 – 2214, 2002.
- [2] S.J. Benson, Y. Ye, and X. Zhang, "Solving large-scale sparse semidefinite programs for combinatorial optimization," *SIAM Journal on Optimization*, vol. 10, no. 2, pp. 443 – 461, 2000.
- [3] S.J. Benson and Y. Ye, "DSDP5: Software for semidefinite programming," *ACM Transactions on Mathematical Software*, 2005.
- [4] S. Burer, R.D.C. Monteiro, and Y. Zhang, "Rank-two relaxation heuristics for Max-Cut and other binary quadratic programs," *SIAM Journal on Optimization*, vol. 12, no. 2, pp. 503 – 521, 2001.
- [5] T. Cui, T. Ho, and C. Tellambura, "Polynomial Moment Relaxation for MIMO Detection," *IEEE International Conference on Communications*, vol. 7, pp. 3129 – 3134, 2006.
- [6] M.O. Damen, H. El Gamal, and G. Caire, "On maximum-likelihood detection and the search for the closest lattice point," *IEEE Transactions on Information Theory*, vol. 49, no. 10, pp. 2389–2402 2003.


 Fig. 17. Average running time, $n = 20$, $m = 15$, QPSK.

- [7] U. Fincke and M. Pohst, "Improved methods for calculating vectors of short length in a lattice, including a complexity analysis," *Mathematics of Computation*, vol. 44, pp. 463 – 471, 1985.
- [8] G.B. Giannakis, Z. Liu, X. Ma, and S. Zhou, "Space-time coding for broadband wireless communications," *Wiley-Interscience*, 1-st ed., 2003.
- [9] J. Jalden, *Detection for multiple input multiple output channels*, Ph.D. Thesis, KTH, School of Electrical Engineering, Stockholm, Sweden, 2006.
- [10] J. Jalden, C. Martin, and B. Ottersten, "Semidefinite programming for detection in linear systems – optimality conditions and space-time decoding", *Proceedings of ICASSP '03*, vol. 4, pp. IV-9 – IV-12, 2003.
- [11] J. Jalden and B. Ottersten, "An exponential lower bound on the expected complexity of sphere decoding," *Proceedings of ICASSP '04*, vol. 4, pp. IV-393 – IV-396, 2004.
- [12] M. Kisiailiou and Z.-Q. Luo, "Probabilistic analysis of semidefinite relaxation for binary quadratic minimization," *SIAM Journal on Optimization*, submitted for publication.
- [13] Z.-Q. Luo, X. Luo, and M. Kisiailiou, "An efficient quasi-maximum-likelihood decoder for PSK signals," *Proceedings of ICASSP '03*, vol. 6, pp. VI 561 – VI 564, 2003.
- [14] Z.-Q. Luo, N.D. Sidiropoulos, P. Tseng, and S. Zhang, "Approximation bounds for quadratic optimization with homogeneous quadratic constraints," *SIAM Journal on Optimization*, vol. 18, no. 1, pp. 1 – 28, 2007.
- [15] W.K. Ma, P.C. Ching, and Z. Ding, "Semidefinite relaxation based multiuser detection for M-ary PSK multiuser systems," *IEEE Transactions on Signal Processing*, vol. 52, no. 10, pp. 2862 – 2872, 2004.
- [16] W.K. Ma, T.N. Davidson, K.M. Wong, Z.-Q. Luo, and P.C. Ching, "Quasi-maximum-likelihood multiuser detection using semi-definite relaxation," *IEEE Transactions on Signal Processing*, vol. 50, no. 4, pp. 912 – 922, 2002.
- [17] Z. Mao, X. Wang, and X. Wang, "Semidefinite programming relaxation approach for multiuser detection of QAM signals," *IEEE Transactions on Wireless Communications*, vol. 6, no. 12, pp. 4275 – 4279, 2007.
- [18] A. Mobasher, M. Taherzadeh, R. Sotirov, and A.K. Khandani, "A near maximum likelihood decoding algorithm for MIMO systems based on semi-definite programming," *Proceedings of International Symposium on Information Theory*, pp. 1686 – 1690, 2005.
- [19] A.D. Murugan, H. El Gamal, M.O. Damen, and G. Caire, "A unified framework for tree search decoding: rediscovering the sequential decoder," *IEEE Transactions on Information Theory*, vol. 52, no. 3, pp. 933 – 953, 2006.
- [20] M. Nekuii, M. Kisiailiou, T.N. Davidson, and Z.-Q. Luo, "Efficient soft demodulation of MIMO QPSK via semidefinite relaxation," submitted to *IEEE Transactions on Signal Processing*, 2008.
- [21] C.P. Schnorr and M. Euchner, "Lattice basis reduction: improved practical algorithms and solving subset sum problems," *Math. Programming*, vol. 66, pp. 181 – 191, 1994.
- [22] N.D. Sidiropoulos and Z.-Q. Luo, "A semidefinite relaxation approach to MIMO detection for higher-order QAM constellations," *IEEE Signal Processing Letters*, vol. 13, pp. 525 – 528, 2006.
- [23] J.F. Sturm, "Using SeDuMi 1.02, a MATLAB toolbox for optimization over symmetric cones," *Optimization Methods and Software*, vol. 11 – 12, pp. 625 – 653, 1999.

- [24] P.H. Tan and L.K. Rasmussen, "The application of semidefinite programming for detection in CDMA," *IEEE Journal on Selected Areas in Communications*, vol. 19, no. 8, pp. 1442 – 1449, 2001.
- [25] K.C. Toh, "A note on the calculation of step-lengths in interior-point methods for semidefinite programming," *Computational Optimization and Applications*, vol. 21, pp. 301 – 310, 1999.
- [26] E. Viterbo and J. Bours, "A universal lattice code decoder for fading channels," *IEEE Transactions on Information Theory*, vol. 45, no. 5, pp. 1639–1642, 1999.
- [27] A. Wiesel, Y. Eldar, and S. Shamai, "Semidefinite relaxation for detection of 16-QAM signaling in MIMO channels," *IEEE Signal Processing Letters*, vol. 12, no. 9, pp. 653–656, 2005.
- [28] Y. Yang, C. Zhao, P. Zhou, and W. Xu, "MIMO detection of 16-QAM signaling based on semidefinite relaxation," *IEEE Signal Processing Letters*, vol. 14, no. 11, pp. 797 – 800, 2007.
- [29] M. Kisiailiou, X. Luo, and Z.-Q. Luo, "Semidefinite relaxation codes for the discrete integer least squares problem," http://www.ece.umn.edu/users/luozq/software/sw_about.html.